Direct Measurement of the Triplet Exciton Diffusion Length in Organic Semiconductors

Mikhnenko, Oleksandr V.; Ruiter, Roald; Blom, Paul W. M.; Loi, Maria Antonietta

Published in:
Physical Review Letters

DOI:
10.1103/PhysRevLett.108.137401

Publication date:
2012

Direct Measurement of the Triplet Exciton Diffusion Length in Organic Semiconductors

Oleksandr V. Mikhnenko,[1,2,*] Roald Ruiter,[1] Paul W. M. Blom,[1,3] and Maria Antonietta Loi[1,†]

[1]*Zernike Institute for Advanced Materials, University of Groningen, Nijenborgh 4, 9747 AG Groningen, The Netherlands*
[2]*Dutch Polymer Institute, P.O. Box 902, 5600 AX, Eindhoven, The Netherlands*
[3]*Holst Centre, High Tech Campus 31, 5605 KN, Eindhoven, The Netherlands*

(Received 23 November 2011; published 29 March 2012)

We present a new method to measure the triplet exciton diffusion length in organic semiconductors. *N*,*N*′-di-[(1-naphthyl)-*N*,*N*′-diphenyl]-1,1′-biphenyl)-4,4′-diamine (NPD) has been used as a model system. Triplet excitons are injected into a thin film of NPD by a phosphorescent thin film, which is optically excited and forms a sharp interface with the NPD layer. The penetration profile of the triplet excitons density is recorded by measuring the emission intensity of another phosphorescent material (detector), which is doped into the NPD film at variable distances from the injecting interface. From the obtained triplet penetration profile we extracted a triplet exciton diffusion length of 87 ± 2.7 nm. For excitation power densities >1 mW/mm^2 triplet-triplet annihilation processes can significantly limit the triplet penetration depth into organic semiconductor. The proposed sample structure can be further used to study excitonic spin degree of freedom.

DOI: 10.1103/PhysRevLett.108.137401 PACS numbers: 78.66.Qn, 71.35.−y, 78.55.Kz, 81.05.Fb

Triplet excitons in organic semiconductors are strongly bound and localized electron-hole pairs that have total electronic spin of one. Diffusion of triplet excitons plays a key role in organic optoelectronic devices: generation of triplet excitons in solar cells using phosphorescent dopants or the process of exciton fission may double the internal quantum efficiency [1,2]. Manipulation of triplet excitons toward phosphorescent emission in light emitting diodes leads to a fourfold increase in the device efficiency [3–5]. In many organic semiconductors the singlet exciton diffusion length is of the order of 10 nm [6], while the triplet diffusion length has been reported in a wide range from 10 to 5000 nm [7–24]. The triplet diffusion length can be measured in a multilayer LED [10–15]. However, in this method the triplet-polaron interactions are neglected in the modeling and it is difficult to evaluate the effect of triplet-triplet annihilation on the resulting values [25]. Other methods include photocurrent modeling [8,16], remote triplet detection in bilayer structures [17,18], variation of exciton profile due to the light penetration depth [19,20], triplet quenching [21], etc. In all of these methods the effect of triplet-triplet annihilation is often neglected.

Even for the same materials quite different triplet diffusion lengths have been published. For instance, in *N*,*N*′-di-[(1-naphthyl)-*N*,*N*′-diphenyl]-1,1′-biphenyl)-4,4′-diamine (NPD) values of 12 and 87 nm have been measured (Ref. [8] and this Letter), in *N*,*N*′-di-1-naphthalenyl–*N*,*N*′ diphenyl-[1,1′: 4′,1″: 4″,1‴-quaterphenyl]-4,4‴-diamine (4P-NPD) of 11 and 54 nm (Refs. [11,13]), in 4,4′-bis(*N*-carbazolyl)biphenyl (CBP) of 16, 25, and 250 nm (Refs. [12,16,17]). Differences in film morphology in these studies may partially be responsible for different values of exciton diffusion length. However, it has been shown for singlet excitons that different film morphologies are characterized by exciton diffusion length within the same order of magnitude [26,27]. Thus the large spread of values for the triplet exciton diffusion length cannot only be justified with the different nature of the molecules studied, but also with the different measurement technique employed.

Here we present a new method to probe triplet exciton diffusion in a prototypical organic semiconductor *N*,*N*′-di-[(1-naphthyl)-*N*,*N*′-diphenyl]-1,1′-biphenyl)-4,4′-diamine (NPD). The proposed multilayer heterostructure has designated triplet injector and triplet detector layers and allows recording the triplet penetration profile into the semiconductor layer. From the obtained profile we extracted a triplet exciton diffusion length of 87 ± 2.7 nm.

NPD, iridium(III)bis(2-(4,6-difluorephenyl)pyridinato-*N*,*C*^{2}) (FIrPic) and meso-tetratolylporphyrin-Pd (PdTPP) were purchased from Sigma-Aldrich, American Dye Source, and Porphyrin Systems, respectively. The materials were used without further purification. Multilayer heterostructures were prepared on quartz substrates by thermal sublimation in high vacuum of less than 2×10^{-7} mbar. The deposition rates of NPD and the metal-organic complexes were kept at ~ 1 Å/s and 0.04 Å/s, respectively. The film thickness was monitored during growth with a quartz microbalance, thickness and surface roughness were controlled after deposition by atomic force microscopy. The root mean square roughnesses of quartz substrates and deposited films were less than 1 nm on an area of 100 μm^2. The samples were handled and stored in a nitrogen atmosphere.

The setup for photoluminescence measurements consisted of an Argon ion laser operating at 466 nm, a monochromator and a photomultiplier tube. The signal was further amplified with a phase sensitive detector. The

samples were mounted in a cryostat and kept under dynamic vacuum at a pressure of 5×10^5 mbar or less, at room temperature. The sample position was varied by shifting the cryostat relative to the optical path using a micrometer actuator. The dependence of the phosphorescence emission on the incident power density was measured using a circular variable neutral density filter and a power meter, which was connected with a computer to record the light intensity directly during the measurements. The Argon laser was detuned from the absorption bands of each material. For instance, the absorption coefficient of NPD is only 2.17×10^{-3} nm^{-1} at the excitation wavelength of 466 nm. Consequently, variations of the exciton density due to optical absorption can be safely neglected in the studied NPD thickness range up to 120 nm. Absorption spectra were measured by a Perkin-Elmer spectrometer under ambient conditions.

Figure 1(a) schematically illustrates the sample structure that we use to measure the triplet exciton diffusion length. An NPD layer of variable thickness L is sandwiched between small amounts of phosphorescent molecules FIrPic and PdTPP; for full names and chemical structures we refer to Fig. 1(c). This 3 layer heterostructure is placed on top of a 50 nm NPD layer that was deposited on a quartz substrate. Accordingly, the NPD-substrate interface does not influence the triplet population in the vicinity of the PdTPP layer. Both phosphorescent materials are sublimed by setting the thickness to 0.4 nm in the vacuum deposition system and they do not form closed layers, as atomic force microscopy reveals (see Supplemental Material [28]). The top layer of FIrPic was applied to only half of the sample area using a shadow mask. We will refer to the two halves of a sample as "FIrPic" and "Reference" sides, indicating whether that side has the FIrPic layer or not.

Figure 1(b) shows the triplet energy levels of FIrPic (Ref. [29]), NPD (Ref. [13]), and PdTPP (deduced from the phosphoresce spectrum). The triplet energy level of NPD is in between that of FIrPic and PdTPP. Therefore it is energetically favorable that triplet excitons get transferred from FIrPic to NPD and subsequently from NPD to PdTPP. As a result, optically excited triplets in the FIrPic can be injected into the NPD layer with thickness L, followed by their diffusion through this layer toward the PdTPP layer, where they are transferred to PdTPP leading to phosphorescent emission.

The PL spectra of the Reference and FIrPic sides of a typical sample are presented in Fig. 2(a). Both spectra feature emission of PdTPP that is identified as pronounced prompt photoluminescence at 620 nm and strong phosphorescence at ~700 and at ~800 nm. The emission at shorter wavelengths is associated with the photoluminescence of NPD. The phosphorescence of the FIrPic layer is too weak to be detected with these measurements. The phosphorescence emission at ~700 nm of the FIrPic side appears to be considerably stronger than that of the Reference side of the sample. The arithmetical difference between these spectra reveals a peak at ~700 nm. The noisy signal at above 750 nm is due to the limitation of the sensitivity range of the photomultiplier tube. For the same reason the enhancement of phosphorescence intensity of the PdTPP emission peak at ~800 nm was difficult to resolve.

The phosphorescence intensity measured at 700 nm of the Reference and FIrPic sides of a typical sample is shown in Fig. 2(b). These spatially resolved data were recorded by scanning through the sample in the direction that is normal to the FIrPic–no FIrPic boundary. The average intensities of I_0 and I_1 correspond to the Reference and FIrPic sides of

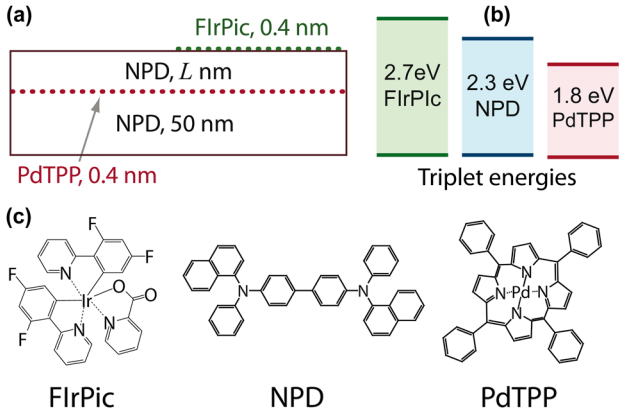

FIG. 1 (color online). Sample structure for triplet exciton diffusion length measurements (a); energy levels of triplet excited states (b); and (c) chemical structures of iridium(III)bis (2-(4 6-difluorephenyl)pyridinato-N,C^2) (FIrPic), N,N'-di-[(1-naphthyl)-N,N'-diphenyl]-1,1′-biphenyl)-4,4′-diamine (NPD), and meso-tetratolylporphyrin-Pd (PdTPP).

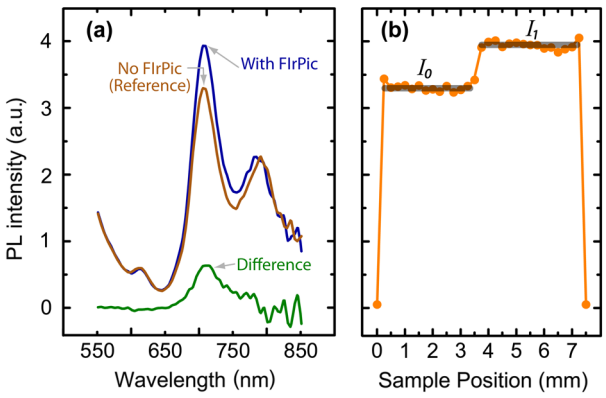

FIG. 2 (color online). (a) Solid lines are photoluminescence spectra of Reference and FIrPic sides of a typical sample used for triplet exciton diffusion measurements. The arithmetical difference between these spectra is also presented. (b) Typical dependence of the phosphorescence emission of PdTPP (detected at 700 nm) depending on the sample spatial position. The average intensities of I_0 and I_1 correspond to the Reference and FIrPic sides of the sample, respectively.

the sample, respectively. The constancy of this signal demonstrates the homogeneity of the sample. Generally, the light outcoupling efficiency of PdTPP emission depends on the NPD layer thickness L. Therefore in order to compare different samples it is convenient to consider the normalized intensity variation:

$$\Delta i = \frac{I_1 - I_0}{I_0}. \quad (1)$$

Figure 3 shows the dependence of Δi on the NPD thickness L. At an excitation power density of 1 mW/mm^2 Δi shows a monoexponential decrease with NPD thickness, while at higher excitation densities the dependence is more complex.

We attribute the increase of the emission intensity Δi to the triplet excitons, which are injected into NPD by FIrPic, diffuse through the layer of thickness L, and are then detected by PdTPP. This increase of intensity cannot be due to the emission of FIrPic, because the two spectra are energetically well separated. Moreover, the small amount of applied FIrPic molecules cannot significantly modify the light outcoupling efficiency or optical interference effects because the refractive indices of NPD and FIrPic are similar and FIrPic form islands of few nanometers that are much smaller than the emission wavelength. Additionally, the intensity increase at 700 nm depends on the NPD thickness L that is consistent with the diffusion of triplet excitons through the NPD layer.

In order to accurately model the process of triplet diffusion in our samples it is important to understand how PdTPP molecules influence the triplet density. Previously, we have studied in detail the detection of triplet excitons using PdTPP as phosphorescent dopant in a material with a band gap similar to NPD [30]. According to the energy gap law, materials of similar band gaps are expected to have a similar triplet lifetime, which is about 0.1 ms for compounds such as NPD at room temperature [30–32]. The phosphorescence decay time of PdTPP is 0.9 ms (Ref. [30]); thus, it takes at least 10 generations of triplet excitons between possible energy transfer events to a PdTPP molecule under continuous wave excitation. Therefore we and others [33] did not detect reduction of triplet lifetime in the host material when doping with PdTPP and similar metal-coordinated porphyrins. Moreover, in our samples PdTPP does not even form a closed layer ensuring a minimal impact on the triplet population and energetic profile in NPD. In this respect PdTPP can be regarded as a triplet detector that does not perturb the density of triplet excitons in the material under investigation.

Because PdTPP behaves as a nonperturbing triplet detector, triplet-triplet annihilation (TTA) can be observed by detecting the phosphorescence of PdTPP. TTA is the bimolecular recombination of two triplet excitons (T_1) that yields singlet ground (S_0) and singlet excited (S_1) states:

$$T_1 + T_1 \rightarrow S_0 + S_1. \quad (2)$$

The efficiency of TTA is only significant if the probability that two triplet excitons meet each other during their lifetime is high. This probability becomes considerable when the triplet density overcomes a certain value. Since the TTA introduces an additional decay path for triplets, their density scales as square root of the generation rate at high excitation powers, while at low triplet generation rates the TTA is inefficient and the scaling is linear [3,34].

Figure 4 shows the dependence of the PdTPP phosphorescence emission intensity on the excitation power density (circles). In this case the 0.4 nm PdTPP layer was sandwiched between two 50 nm thick layers of NPD. The dependence shows slopes of 1 and 0.54 on the log-log scale at low and high excitation densities, respectively. In

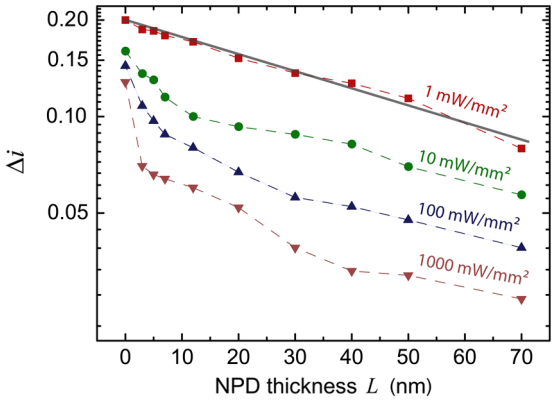

FIG. 3 (color online). Normalized variation of the phosphorescence intensity at 700 nm (Δi) vs NPD layer thickness L. Samples were excited at 466 nm; various excitation power densities are presented. The dashed lines serve as guides to the eye; the solid line is a fit with Eq. (4).

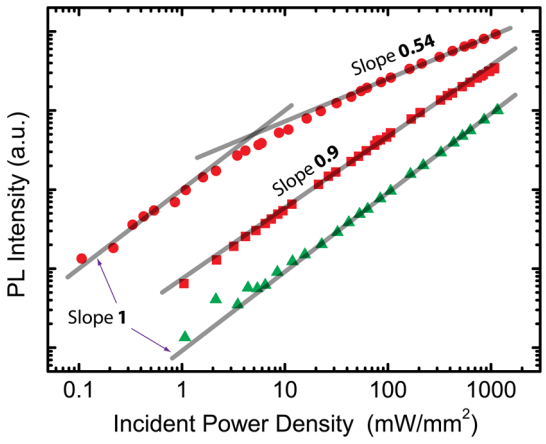

FIG. 4 (color online). The dependence of the emission intensity on the incident power density in a NPD-PdTPP-NPD heterostructure at 700 nm (circles) and at 550 nm (triangles); in PdTPP-polystyrene blend at 700 nm (squares). Laser excitation was at 466 nm.

contrast, the prompt photoluminescence of NPD scales linearly within the whole studied range of the excitation densities (triangles). As a further check we measured the phosphorescence emission of PdTPP molecules in the inert matrix of polystyrene and also this sample shows a nearly linear dependence on the excitation power (squares in Fig. 4). Thus the sublinear growth with the scaling exponent of 0.54 measured at high excitation power is specific to the PdTPP-NPD heterojunction. In our previous work we associated such square root dependence to the detection of triplet excitons under TTA conditions [30]. Consequently, the phosphorescence emission of PdTPP is mainly determined by the triplet excitons, which were created via intersystem crossing in NPD layers and transferred to PdTPP.

At the excitation power density of 1 $\mathrm{mW/mm^2}$ the phosphorescence intensity at 700 nm is in the linear regime (Fig. 4). Thus the TTA process is not efficient at this excitation power and diffusion of triplets that are injected by FIrPic can be modeled by a linear differential equation. At room temperature the triplet exciton diffusion can be described in terms of normal diffusion [35]. Because of the sample symmetry, the density n of injected triplet excitons depends only on one spatial coordinate L that is the distance from the FIrPic-NPD interface:

$$\frac{\partial n}{\partial t} = D\frac{\partial^2 n}{\partial L^2} - \frac{n}{\tau} + G(L), \tag{3}$$

where $n \propto \Delta i$, D is the diffusion coefficient, and τ is the triplet lifetime. Upon continuous wave laser excitation the triplet generation rate $G(L)$ can be replaced by a boundary condition $n(0, t) = G_0$ at the FIrPic-NPD interface. Then the thickness profile of the triplet penetration into NPD layer is the steady state solution of Eq. (3) and can be easily found by setting $\partial n/\partial t = 0$:

$$n(L) = G_0 e^{-L/L_D}, \tag{4}$$

where $L_D = \sqrt{\tau D}$ is the exciton diffusion length—the only fitting parameter. The solid line in Fig. 3 is the fitting with Eq. (4) that yields to the exciton diffusion length of 86.8 ± 2.7 nm; the error is the standard error of the fitting parameter. The triplet exciton diffusion coefficient D can be estimated by setting $\tau = 0.1$ ms resulting in the value of 7.5×10^{-7} $\mathrm{cm^2/s}$.

Under intense laser excitation TTA becomes significant (see Fig. 4) and the profile of triplet penetration cannot be described with Eq. (4). In this case the triplet density within the FIrPic side of the sample is given by

$$\frac{\partial n}{\partial t} = D\frac{\partial^2 n}{\partial L^2} - \frac{n}{\tau} - \gamma n^2 + G(L), \tag{5}$$

where γ is the triplet-triplet annihilation rate [3,34]. Here it is important to account also for the triplet excitons that are generated via intersystem crossing within the NPD layer. Thus the triplet generation rate can be written as

$$G(L) = G_0\delta(L) + g(L), \tag{6}$$

where $\delta(L)$ is a delta function, $g(L)$ is the triplet generation rate within the NPD layer due to intersystem crossing. Generally speaking, $g(L)$ depends on the optical interference effects due to the variation of the NPD thickness. For this reason it is not straightforward to solve Eq. (5). Nevertheless, we expect that under intense excitation the triplet penetration profile $n(L)$ will be a steeper function in the vicinity of the injector layer. Indeed, Fig. 3 shows this effect at excitation powers of 10 $\mathrm{mW/mm^2}$ and higher.

In order to compare the different profiles in Fig. 3 we define the penetration depth λ as the distance from the FIrPic-NPD interface at which the concentration of injected triplets is attenuated by a value of e^{-1}. The value of λ systematically decreases from 87 nm to 67, to 39, and to 24 nm when the excitation power densities is increased from 1 $\mathrm{mW/mm^2}$ to 10, to 100, and to 1000 $\mathrm{mW/mm^2}$ in accordance with TTA [17]. Thus it is important to make sure that TTA is absent or it is taken into account in the measurement of triplet exciton diffusion length, because the penetration length λ can be mistakenly interpreted as the diffusion length L_D. Presumably, this may be the reason of the large spread in L_D values that were reported in the literature for the same materials; in those experiments the effect of TTA was usually neglected [8,11–13,16].

The proposed sample structure with distinct triplet injector and detector layers can be further developed to explore the spin degree of freedom of triplet excitons. In particular, the influence of the magnetic field on the triplet diffusion length and triplet-triplet annihilation can be observed. The magnetic field may significantly decrease the efficiency of the triplet-triplet annihilation and consequently increase the triplet penetration depth at high excitation densities. New types of devices may emerge by using the spins of triplet excitons.

In summary, we presented a new direct method to accurately measure triplet exciton diffusion lengths in organic semiconductors. A triplet exciton diffusion length of 86.8 ± 2.7 nm was extracted for NPD. Our method can be applied to a wide selection of materials that are relevant for applications as OLEDs and solar cells. We have also shown that triplet-triplet annihilation effects can significantly reduce the penetration depth of triplet excitons, being detrimental for the eventual use of triplet excitons in optoelectronic devices.

The authors thank Dr. V. Krasnikov for the useful discussions; F. v.d. Horst, A. Kamp, J. Harkema, and H. M. M. Hesp for the technical support. The work of O. V. M. is a part of the research program of the Dutch Polymer Institute (Project No. 518). The sample preparation has been performed at NanoLab Groningen.

*Corresponding author.
alex@mikhnenko.com
†Corresponding author.
m.a.loi@rug.nl

[1] Akshay Rao, Mark W. B. Wilson, Justin M. Hodgkiss, Sebastian Albert-Seifried, Heinz Bassler, and Richard H. Friend, J. Am. Chem. Soc. **132**, 12 698 (2010).
[2] Chang-Lyoul Lee, In-Wook Hwang, Clare Chisu Byeon, Bok Hyeon Kim, and Neil C. Greenham, Adv. Funct. Mater. **20**, 2945 (2010).
[3] A. Köhler and H. Bässler, Mater. Sci. Eng., R **66**, 71 (2009).
[4] Yiru Sun, Noel C. Giebink, Hiroshi Kanno, Biwu Ma, Mark E. Thompson, and Stephen R. Forrest, Nature (London) **440**, 908 (2006).
[5] Sebastian Reineke, Frank Lindner, Gregor Schwartz, Nico Seidler, Karsten Walzer, Bjorn Lussem, and Karl Leo, Nature (London) **459**, 234 (2009).
[6] Peter Peumans, Aharon Yakimov, and Stephen R. Forrest, J. Appl. Phys. **93**, 3693 (2003).
[7] Barry P. Rand, Claudio Girotto, Alexander Mityashin, Afshin Hadipour, Jan Genoe, and Paul Heremans, Appl. Phys. Lett. **95**, 173304 (2009).
[8] Wade A. Luhman and Russell J. Holmes, Appl. Phys. Lett. **94**, 153304 (2009).
[9] J. E. Kroeze, R. B. M. Koehorst, and T. J. Savenije, Adv. Funct. Mater. **14**, 992 (2004).
[10] Wei Zhang, Junsheng Yu, Wen Wen, and Yadong Jiang, J. Lumin. **131**, 1260 (2011).
[11] J. Wünsche, S. Reineke, B. Lüssem, and K. Leo, Phys. Rev. B **81**, 245201 (2010).
[12] M. Lebental, H. Choukri, S. Chenais, S. Forget, A. Siove, B. Geffroy, and E. Tutis, Phys. Rev. B **79**, 165318 (2009).
[13] Gregor Schwartz, Sebastian Reineke, Thomas Conrad Rosenow, Karsten Walzer, and Karl Leo, Adv. Funct. Mater. **19**, 1319 (2009).
[14] M. A. Baldo and S. R. Forrest, Phys. Rev. B **62**, 10958 (2000).
[15] M. A. Baldo, D. F. O'Brien, M. E. Thompson, and S. R. Forrest, Phys. Rev. B **60**, 14422 (1999).
[16] Noriyuki Matsusue, Satoshi Ikame, Yuichiro Suzuki, and Hiroyoshi Naito, J. Appl. Phys. **97**, 123512 (2005).
[17] N. C. Giebink, Y. Sun, and S. R. Forrest, Org. Electron. **7**, 375 (2006).
[18] Toshiki Fushimi, Akimichi Oda, Hideo Ohkita, and Shinzaburo Ito, J. Phys. Chem. B **108**, 18897 (2004).
[19] H. Najafov, B. Lee, Q. Zhou, L. C. Feldman, and V. Podzorov, Nature Mater. **9**, 938 (2010).
[20] Richard R. Lunt, Noel C. Giebink, Anna A. Belak, Jay B. Benziger, and Stephen R. Forrest, J. Appl. Phys. **105**, 053711 (2009).
[21] Mohammad Samiullah, Dhanashree Moghe, Ullrich Scherf, and Suchi Guha, Phys. Rev. B **82**, 205211 (2010).
[22] Yichun Luo and Hany Aziz, J. Appl. Phys. **107**, 094510 (2010).
[23] Jessica E. Kroeze, Tom J. Savenije, Luis P. Candeias, John M. Warman, and Laurens D. A. Siebbeles, Solar Energy Mater. Sol. Cells **85**, 189 (2005).
[24] M. A. Baldo, C. Adachi, and S. R. Forrest, Phys. Rev. B **62**, 10 967 (2000).
[25] N. C. Giebink and S. R. Forrest, Phys. Rev. B **77**, 235215 (2008).
[26] Seung-Bum Rim, Reinhold F. Fink, Jan C. Schoneboom, Peter Erk, and Peter Peumans, Appl. Phys. Lett. **91**, 173504 (2007).
[27] Richard R. Lunt, Jay B. Benziger, and Stephen R. Forrest, Adv. Mater. **22**, 1233 (2010).
[28] See Supplemental Material at http://link.aps.org/supplemental/10.1103/PhysRevLett.108.137401 for atomic force microscopy images of the sample surface.
[29] Qi Wang, Junqiao Ding, Dongge Ma, Yanxiang Cheng, Lixiang Wang, Xiabin Jing, and Fosong Wang, Adv. Funct. Mater. **19**, 84 (2009).
[30] Oleksandr V. Mikhnenko, Paul W. M. Blom, and Maria Antonietta Loi, Phys. Chem. Chem. Phys. **13**, 14 453 (2011).
[31] Chang-Lyoul Lee, Xudong Yang, and Neil C. Greenham, Phys. Rev. B **76**, 245201 (2007).
[32] J. Kalinowski, W. Stampor, M. Cocchi, D. Virgili, V. Fattori, and P. Di Marco, Chem. Phys. **297**, 39 (2004).
[33] P. A. Lane, L. C. Palilis, D. F. O'Brien, C. Giebeler, A. J. Cadby, D. G. Lidzey, A. J. Campbell, W. Blau, and D. D. C. Bradley, Phys. Rev. B **63**, 235206 (2001).
[34] V. Dyakonov, G. Rösler, M. Schwoerer, and E. L. Frankevich, Phys. Rev. B **56**, 3852 (1997).
[35] Vygintas Jankus, Chris Winscom, and Andrew P Monkman, J. Phys. Condens. Matter **22**, 185802 (2010).